Time-Frequency Analysis of Superorbital Modulation of X-ray Binary SMC X-1 by Hilbert-Huang Transform

Chin-Ping Hu[1], Yi Chou[1], Ming-Chya Wu[2], Ting-Chang Yang[1], Yi-Hao Su[1]

1 Institute of Astronomy, National Central University, Taiwan
2 Research Center for Adaptive Data Analysis, National Central University, Taiwan

Abstract

The high-mass X-ray binary (HMXB) SMC X-1 exhibits a superorbital modulation with a dramatically varying period ranging between ~40 d and ~60 d. This research studies the time-frequency properties of the superorbital modulation of SMC X-1 based on the observations made by the All-Sky Monitor (ASM) onboard the Rossi X-ray Timing Explorer (RXTE).We analyzed the entire ASM database collected since 1996. The Hilbert-Huang Transform (HHT), developed for non-stationary and nonlinear time series analysis, was adopted to derive the instantaneous superorbital frequency. The resultant Hilbert spectrum is consistent with the dynamic power spectrum while it shows more detailed information in both the time and frequency domains. The RXTE observations manifest that the superorbital modulation period was mostly betweenn~50 d and ~65 d, whenas it changed to ~45 d around MJD 50,800 and MJD 54,000. Our analysis further indicates that the instantaneous frequency changed in a time scale of hundreds of days between ~MJD 51,500 and ~MJD 53,500. Based on the instantaneous phase defined by HHT, we folded the ASM light curve to derive a superorbital profile, from which an asymmetric feature and a low state with barely any X-ray emissions (lasting for ~0.3 cycles) were observed. We also calculated the correlation between the mean period and the amplitude of the superorbital modulation. The result is similar to the recently discovered relationship between the superorbital cycle length and the mean X-ray flux for Her X-1.

1. Introduction

The high-mass X-ray binary (HMXB) SMC X-1, which was first discovered in 1971 (Leong et al. 1971), consists of a 1.06 M⊙ neutron star (van der Meer at al. 2007) and a B0 I type supergiant with a mass of 17.2 M⊙. The spin period of the neutron star is 0.71 s (Wojdowski et al. 1998) and the orbital period of this system is ~3.89 d as evaluated by its eclipse (Schreier et al. 1972).

SMC X-1 exhibits a superorbital modulation with its period changes between ~40 d and ~65 d. After the All-Sky Monitoring (ASM) onboard the Rossi X-ray Timing Explorer (RXTE) collected sufficient amounts of data, several time-frequency analysis methods such as the wavelet transform (Ribó et al. 2001), dynamic power spectrum (Clarkson et al. 2003), and sliding Lomb-Scargle periodogram (Trowbridge et al. 2007) were applied to the light curve to investigate the variations in the superorbital period of SMC X-1. The mechanism of superorbital modulations in SMC X-1 are interpreted by a warped and tilted accretion disk (Wojdowski et al. 1998). When the disk precesses, it obscures our line of view to the central X-ray source.

2. Data Analysis

2.1 RXTE ASM

Since the RXTE was launched in late 1995, the ASM continuously sweeps the entire sky once every 90 minutes. The energy range of the ASM is 1.3 to 12.1 keV. This can be further divided into three energy channels (ch1: 1.3-3.0 keV, ch2: 3.0-5.0 keV, and ch3: 5.0-12.1 keV). The summed band data collected from 1996 to 2010 (MJD 50134 to MJD 55371), with a total time span of ~5000 d were used in this time-frequency analysis. The dwell data, where all the eclipses were removed according to the ephemeris proposed by Wojdowski et al. 1998, were binned into a one-day averaged light curve.

2.2 Hilbert-Huang Transform

Owing to the high variability of the superorbital cycle length of SMC X-1, it is suitable to analyze the time-frequency properties of its superorbital modulation by the HHT. HHT, established in 1998 (Huang et al. 1998), is an adaptive data analysis method that can detect the frequency changing with time instantaneously. The procedure of HHT is divided into two steps: decomposing the original data into intrinsic mode functions (IMFs) and applying Hilbert transform or other method on the IMFs to obtain the instantaneous frequencies and amplitudes. Thus, the original light curve x(t) can be represented as:

$$x(t) = \sum_{j=1}^{n} a_j(t) \exp\left(i \int_0^t \omega_j(t')dt' \right)$$

where $a_j(t)$ and $\omega_j(t)$ are the instantaneous amplitudes and frequencies of decomposed components.

The RXTE/ASM lightcurve was decomposed into IMFs by Ensemble Empirical Mode Decomposition (EEMD) method (Wu et al. 2009). The decomposition result is shown as Figure 1. The significance test (Wu et al. 2004) on these IMFs suggests that the 40 -- 60 d superorbital modulation signal of SMC X-1 mostly concentrates in the fifth component (c_5). The values of all the other components are lower than or marginal at the 3σ white noise level, suggesting that they act in a manner similar to white noise. These components are probably caused by the observational noise associated with non-periodic modulations in other time scales.

3. Result

3.1 Hilbert Spectrum

After decomposing the ASM light curve into IMFs, the normalized Hilbert transform (Huang & Long 2003} was applied on the IMFs to obtain the instantaneous frequencies and amplitudes. The resultant Hilbert spectrum is a three-dimensional map which displays how the modulation period and amplitude vary with time. Figure 2 shows the result, in which the frequency range is divided into 3000 bins and the spectrum is smoothed by a Gaussian filter for clarity. The color map represents the Hilbert energy spectrum with the magnitude of energy defined as square of the amplitude. For comparison, the dynamic power spectral technique, as described in Clarkson et al. (2003), was also applied on the ASM light curve. It is obvious that the Hilbert energy spectrum is consistent with the dynamic power spectrum. Because the spectral analysis based on HHT is independent of window size, more detailed structures in the light curve data can be observed from the high-resolution Hilbert spectrum than the dynamic power spectrum.

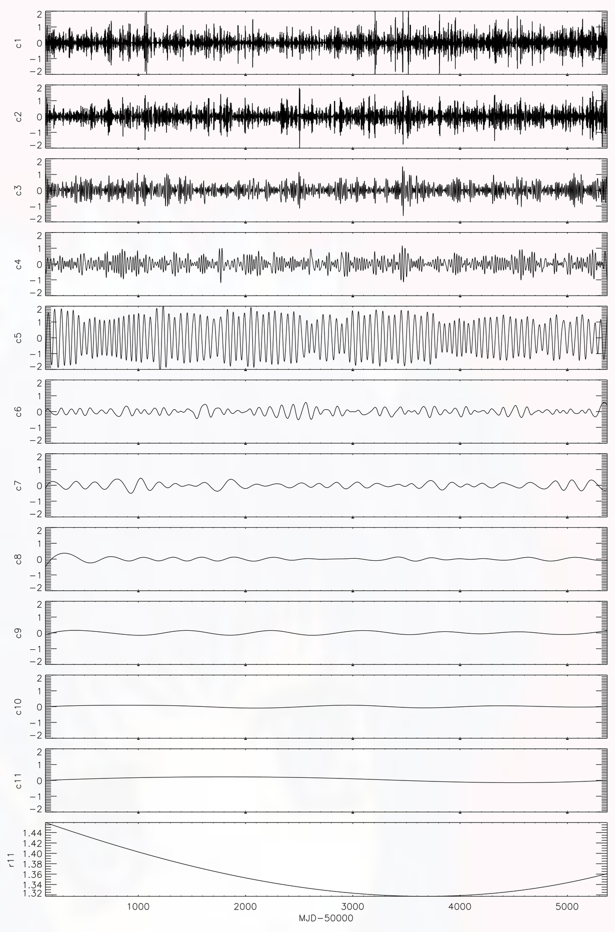

Figure 1. Intrinsic mode functions (IMFs) decomposed by ensemble empirical mode decomposition (EEMD). The fifth IMF (c_5) is responsible for the ~40 d to ~60 d superorbital modulation.

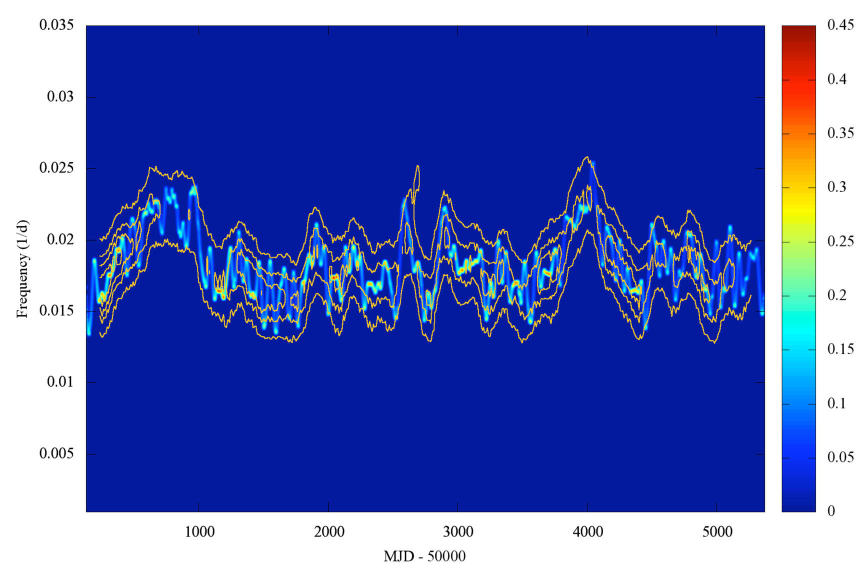

Figure 2. Hilbert energy spectrum (color map) and dynamic power spectrum (contour plot). The blue curve represents the instantaneous frequency of IMF c_5 after Gaussian smoothing and the color depth denotes the magnitude of the Hilbert energy.

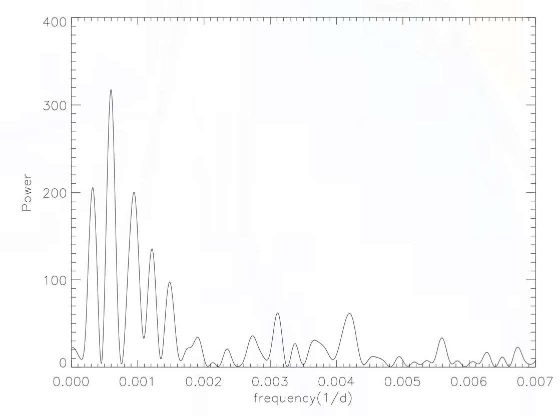

Figure 3. Lomb-Scargle periodogram of the instantaneous frequency of IMF c_5. The highest peak is located at f~.0006 (or P=1647 d), which is the second harmonic of P~3200 d peak. The other prominent peaks are located at P~240 d d and P~320 d.

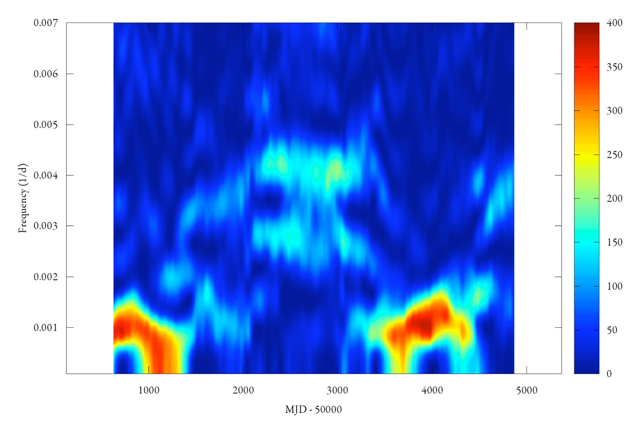

Figure 4. Dynamic power spectrum of the instantaneous frequency of IMF c_5.

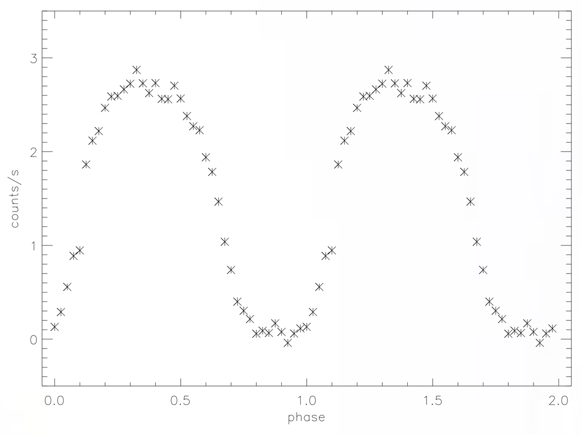

Figure 5. Folded light curve of SMC X-1 according to the phase defined by HHT. The number of bins in one cycle is 40.

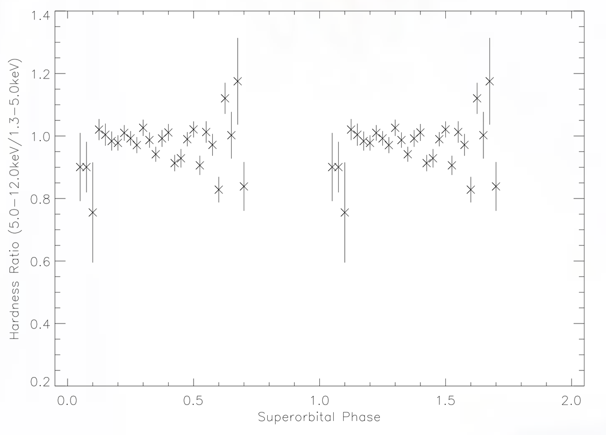

Figure 6. Hardness ratios folded according to the superorbital phase. Only the data points with a signal to noise ratio greater than 5 were chosen to calculate the hardness ratios.

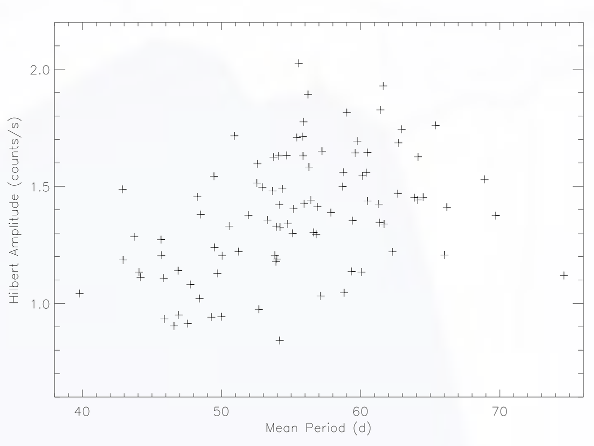

Figure 7. Correlation of cycle-averaged period and Hilbert amplitude of IMF c_5.

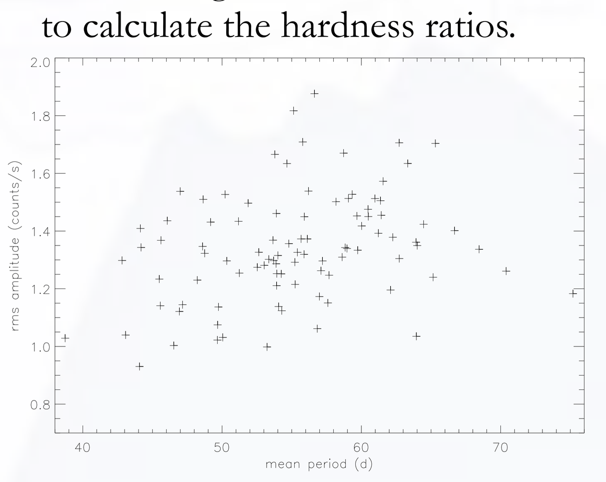

Figure 8. Correlation of cycle-averaged period and rms amplitude of original ASM light curve.

The first remarkable feature of both spectra is that the superorbital modulation period changes dramatically from ~60 d to ~45 d and goes back to ~60 d between ~MJD 50,200 and ~MJD 51,100. Interestingly, a similar variation in the superorbital modulation period is repeated between ~MJD 53,600 and ~MJD 54,400. The time durations of these two events are roughly 800 d and the separation between them is ~3200 d. This indicates that such a phenomenon is probably recurrent. In addition, although the superorbital period is relatively stable, it seems to oscillate between P ~ 50 d and~65 d over a time scale of hundreds of days between ~MJD 52,000 and ~MJD 53,000. The Hilbert spectrum displays the instantaneous frequency more accurately, enabling the application of further timing analysis methods on the instantaneous frequency to assess the periodicity hidden in the superorbital period change.

In order to study the periodicities in the variation of the superorbital frequency, the Lomb-Scargle periodogram was applied on the instantaneous frequency of the component c_5, and the result is shown in Figure 3. The highest peak is located at P = 1674 d; this is consistent with the previously reported periodicity (Ribó et al. 2001, Clarkson et al. 2003). However, this peak is the second harmonic of P ~ 3200 d, and it corresponds to the separation of the events occurring when the superorbital period changes between ~60 d and ~45 d. Moreover, a few peaks with relatively less power values located at P ~ 240 d and P ~ 320 d are observed. Figure 4 shows a dynamic power spectrum with a window size of 1,000 d and a movement of 10 d. The most prominent peaks are located at around MJD 50,800 and MJD 54,000. These peaks correspond to the short-period state of the superorbital modulation in the time domain in Figure 2 and the highest peaks in the frequency domain in Figure 3.

3.2 Superorbital Profile

It is difficult to derive a proper profile to describe the characteristics of superorbital modulation for highly variable cycle lengths from a light curve folded with a fixed period. From Hilbert transform, a well-defined phase of $\phi(t)=\theta(t)/2\pi$ can be easily obtained even if the period changes dramatically. Figure 5 shows the folded light curve of SMC X-1, and the phase zero epoch is defined by the first data point in the light curve (MJD 50,134).

The major distinction between this superorbital modulation profile and that obtained from previous studies is a clear low state with a negligible X-ray flux lasting for ~0.3 cycle. Moreover, the asymmetric features of the superorbital profile can also be obtained in the folded light curve. By calculating the time scale between 10% and 90% of amplitude, the rising time scale is ~0.14 cycle (from phase 0.05 to 0.19), which is shorter than the falling time scale of ~0.19 cycle (from phase 0.54 to 0.73).

The ASM hardness ratio was defined as ch3/(ch1+ch2), since ch3 and ch1+ch2 have similar photon count rates during the high state. Only the data with a signal to noise ratio (SNR) greater than 5 were chosen and folded according to the superorbital phase defined in HHT. The folded hardness ratio is shown in Figure 6. It is easily observed that the hardness ratios in the high state (from phase 0.19 to 0.54) are relatively stable. In the transition state (phase 0.05--0.19, and 0.54--0.73), the hardness ratios do not appear to significantly deviate from the mean value as compared with that in the high state although the errors are much greater.

3.3 Correlation Between Period and Amplitude

Another remarkable feature observed in this study is the correlation of the amplitude with the period. Using the instantaneous frequency and amplitude derived by HHT, the correlation between the cycle-averaged period and the Hilbert amplitude in the most significant IMF (c_5) was calculated. The rank correlation coefficient is r=0.46 with a null hypothesis probability value of 3.2×10^{-6}, indicating a significant correlation between the period and the amplitude (see Figure 7). In order to obtain the correlation between the period and amplitude in the original data set, the rms amplitude of each cycle was calucalted. The result shows that the period and the rms amplitude still show a significant correlation (r=0.32 with null hypothesis probability value of 1.4×10^{-3}, see Figure 8).

4. Summary

We have successfully performed HHT-based time-frequency analysis on the ASM light curve of SMC X-1. The Hilbert spectrum manifests variations in the instantaneous period of the superorbital modulation. The instantaneous phase defined by HHT allows us to fold the light curve to derive a reasonable superorbital profile. The time-frequency information obtained from the HHT analysis is more abundant than the traditional Fourier-based methods. This benefits our investigations on the superorbital modulation of SMC X-1.

References

Clarkson, W. I., et al. 2003, MNRAS, 339, 447
Hickox, R. C., & Vrtilek, S. D. 2005, ApJ, 633, 1064
Huang, N. E. et al. 1998. Proc. R. Soc. Lond. A, 454, 903
Huang, N. E., & Long, S. R. 2003, NASA Patent Pending GSC 14,673-1
Leong, C., et al. 1971, ApJ, 170, L67
Neilsen, J., et al. 2004, ApJ, 616, L135
Reynolds, A. P., et al. 1993, MNRAS, 261, 337
Ribó , M., et al. in Proc. of Fourth INTEGRAL Workshop
Schreier, E., et al, 1972, ApJ, 178, L71
Trowbridge, S., et al. 2007, ApJ, 670, 624
van der Meer, A., et al. 2007, A&A, 473, 523
Wojdowski, P., et al. 1998, ApJ, 502, 253
Wu, Z., & Huang, N. E. 2004, Proc. R. Soc. Lond. A, 460, 1597
Wu, Z., & Huang, N. E. 2009, Advance in Adaptive Data Analysis, vol 1, 1, 1